Desalination and Water Treatment
www.deswater.com

doi: 10.5004/dwt.2022.28491

262 (2022) 190–199
June

Extraction of scandium from aqueous solution in a rotating microchannel reactor

Duan Liu, Gaoxiang Chen, Zini Guo, Sanxing Li, Jianhong Luo*

School of Chemical Engineering, Sichuan University, Chengdu, Sichuan 610065, China,
emails: luojianhong@scu.edu.cn (J. Luo), 2691631314@qq.com (D. Liu), yunhaoccc@163.com (G. Chen), guozn97@163.com (Z. Guo), lsx_nfyf@163.com (S. Li)

Received 11 July 2021; Accepted 27 March 2022

ABSTRACT

Scandium, as a typical dispersed element, plays an important role in modern technology. The liquid–liquid microextraction of scandium from an aqueous solution is carried out with $C_{16}H_{35}O_3P$ (EHEHPA) as the extraction agent with kerosene as the diluent. The effects of pH of an aqueous solution, outer-inner rotor distance (D), the height of inner rotor (H), speed of the inner rotor (R), the flow velocity of the organic phase (Q_O), and the ratio of organic phase to the aqueous phase (O/A) on extraction efficiency, mass transfer coefficient and equilibrium mechanism of Sc^{3+} are analyzed investigated. The results of this study revealed that the removal rate of Sc^{3+} in the aqueous phase reaches more than 97%. To investigate the influence of NaOH concentration on the extraction process, NaOH solution is selected as a stripping agent for reverse extraction of the loaded organic phase.

Keywords: Scandium; Microextraction; $C_{16}H_{35}O_3P$; Liquid–liquid

1. Introduction

Scandium is a rare earth element that is principally used in all walks of life, such as optical, aluminum-scandium alloys and automotive industries due to its excellent alloying and electrical properties [1,2]. Lots of work has been done on the recovery and separation of scandium from secondary resources including various industrial residues, tailings and waste liquors by solvent extraction, ion exchange adsorption and precipitation, etc. [3–5]. In recent years, solvent extraction has been widely used in the separation of rare earth elements and impurities for its advantages of large capacity, simple operation and high selectivity [6]. However, the current extraction technology is inefficient for the extraction of scandium. Besides, solvent extraction still has some limitations of long operation time and poor mass transfer performance [7].

Microfluidic technology is a new technology based on the microreactor and microchannel. Many studies have validated that the combination of microfluidic technology and solvent extraction can greatly improve the transfer efficiency of liquid–liquid two phases[8,9]. Liquid–liquid extraction in microchannels has attracted more and more attention because of its high overall volumetric mass transfer coefficient, narrow drop size distributions and short residence time [10–12]. The driving force of the mass and heat transfer process gets intensified due to the small diffusion distance and characteristic size within a range of hundreds of micrometers[13,14]. In addition, the microchannel can provide a large contact area for the liquid–liquid two phases, which can significantly improve the reaction selectivity. The residence time of fluids in the microchannel can be controlled precisely by changing the operating parameters such as flow velocity and length of the microchannel, so that the liquid–liquid two-phase fluids can be fully mixed in a short time [15–18]. Microchannel reactors can be divided into active and passive mixing types according to the mixing mode. Active mixing

* Corresponding author.

requires external energy such as electric field, temperature field and so on, while passive mixing is accomplished entirely by diffusion or convection of the liquids within the microchannel such as Y-junction [19], T-junction [20] and other microchannels. Ma et al. [21] has studied the effect of smooth and engraved inner rotors on the extraction performance in a rotating microchannel extractor (RME). The results has been shown that the extraction equilibrium is broken under certain conditions. Darekar et al. [22] has extracted uranium with tributyl phosphate (TBP) using a T-junction microchannel reactor and studied the effects of residence time, the ratio of organic to aqueous phases (O/A) and microchannel diameters on the extraction performance. The results hae been revealed that the total mass transfer coefficient decreases with the increased residence time and increases with the decrease of O/A. Yin et al. [23] has found that the extraction efficiency of lanthanum reaches nearly 100% in the residence time of 0.37s using a Y-junction glass microchannel reactor. Chen et al. [24] has realized that the rapid separation of rare earth elements by using a droplet microreactor and the extraction efficiency increases significantly with the increase of residence time.

In this work, we used a homemade rotating microchannel reactor that met the standards of microchannel devices [25]. The inner rotor was driven to rotate by the electric motor of the microchannel reactor, which provided external force for active mixing of liquid–liquid two phases. In this work, $C_{16}H_{35}O_3P$ (EHEHPA) was used as the extractant to extract scandium from the scandium nitrate solution. In this work, a certain reference value for future research was supplied for the microchannel reactor with active type.

2. Experimental

2.1. Materials

The diluent was sulfonated kerosene bought from Chengdu Jinshudu Laboratory Equipment Co., Ltd., China (AR grade). $C_{16}H_{35}O_3P$ (EHEHPA) was used as the extractant produced by Luoyang Zhongda Chemical Co., Ltd., China (AR grade). Scandium nitrate hexahydrate was bought from Shanghai Aladdin Biochemical Technology Co., Ltd., China (AR grade). Deionized water was homemade in the laboratory.

2.2. Experimental procedure

The schematic diagram of the experimental setup is presented in Fig. 1. The equipment is composed of two syringe pumps (LSP01-2A, Baoding Langer Constant Current Pump Co., Ltd), a motor (51K60RA-CF, Suzhou Oubang Precision Motor Co., Ltd.), an outer cylinder, and an inner rotor. The inner rotor is made of Teflon which is designed to be hydrophobic while the outer cylinder is made of organic glass designed to be hydrophilic, to observe the flow patterns of liquids in the rotating microchannel reactor. At the same time, different hydrophilicity can avoid the emulsification of the organic phase and aqueous phase.

Driven by the syringe pump, the organic and aqueous phases enter the microchannel reactor from the lower inlet. The stainless steel shaft drives the inner rotor to rotate under the action of the motor, then the liquid–liquid two-phase mass transfer process will happen in the microchannel reactor. The mixed phases are discharged from the upper outlet and then flow into the separating funnel through the pipe. There will be a noticeable phenomenon that the organic phase is on the upper and the aqueous phase is on the lower due to density in 10 min.

2.3. Experimental conditions

The organic phase was consisted of sulfonated kerosene as the solvent and EHEHPA as the extractant with a volume ratio of 49:1. The aqueous phase was composed of a scandium nitrate solution in which the concentration of scandium was 470 mg/L. Besides, the initial pH of the

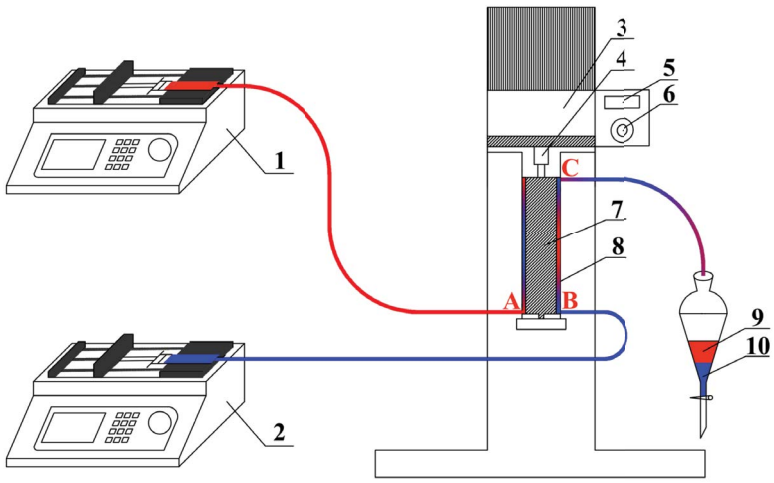

Fig. 1. Schematic diagram of experimental setup: (1) Aqueous syringe pump; (2) Organic syringe pump; (3) Motor; (4) Stainless steel shaft; (5) Speed digital display screen; (6) Speed regulator; (7) Inner rotor; (8) Outer cylinder; (9) Organic phase; (10) Aqueous phase; (A) Inlet of organic phase; (B) Inlet of aqueous phase; (C) Outlet of the mixed phases.

aqueous phase was 3.50. The phase ratio of organic phase to the aqueous phase (O/A) was 2:5. In this experiment, the rotating microchannel reactor was operated at atmospheric pressure and room temperature.

The structure diagram of the rotating microchannel reactor is illustrated in Fig. 2. In this work, the outer cylinder with an inner diameter of 19.6 mm was attached under the motor. The size of the rotating microchannel reactor was controlled by replacing the inner rotor of different diameters (18.9 and 19.1 mm) and heights (100 and 200 mm). The speed (R) of inner rotor was controlled at the range of 0 to 800 rpm, and the flow velocity of the organic phase (Q_O) ranged from 0.16 to 1.60 mL/min.

2.4. Physical properties and analysis

The residual concentration of scandium, from the aqueous phase of the separating funnel, was analyzed by the absorbance value at the wavelength of 649 nm using a visible light spectrophotometer (UV-1100, Shanghai Mapada Instruments Co., Ltd.). The linear equation of the standard curve (Y = 0.0534X–0.0001, the correlation coefficient is 0.9991) was obtained in the experiment to determine the concentration of scandium in the aqueous phase.

3. Results and discussions

Eqs. (1)–(8) given below are often used to analyze the experimental results [26].

The value of percentage stage efficiency η reflects the extraction performance and is defined as follows:

$$\eta = \frac{C_{O,o} - C_{O,i}}{C^*_{O,e} - C_{O,i}} \times 100\% \tag{1}$$

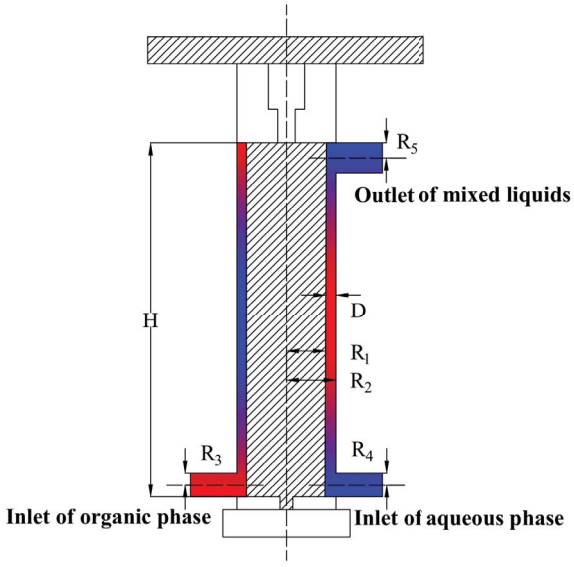

Fig. 2. Structure diagram of the rotating microchannel reactor: (R_1) 9.45~9.55 mm; (R_2) 9.8 mm; (R_3) 1 mm; (R_4) 1 mm; (R_5) 2 mm; (D) 0.25~0.35 mm; (H) 100~200 mm.

The percentage extraction E can be expressed as follows:

$$E = \frac{C_{A,i} - C_{A,o}}{C_{A,i}} \times 100\% \tag{2}$$

The mean mass transfer flux ($\bar{N}$) can be defined as follows:

$$\bar{N} = \frac{Q_O\left(C_{O,o} - C_{O,i}\right)}{Va} \tag{3}$$

Δ_{LMC} is a log mean concentration difference defined as follows:

$$\begin{aligned}\Delta_{LMC} &= \frac{\left(C^*_{O,i} - C_{O,i}\right) - \left(C^*_{O,o} - C_{O,o}\right)}{\ln\left\{\left(C^*_{O,i} - C_{O,i}\right)/\left(C^*_{O,o} - C_{O,o}\right)\right\}} \\ &= \frac{\left(K_d C_{A,i} - C_{O,i}\right) - \left(K_d C_{A,o} - C_{O,o}\right)}{\ln\left\{\left(K_d C_{A,i} - C_{O,i}\right)/\left(K_d C_{A,o} - C_{O,o}\right)\right\}}\end{aligned} \tag{4}$$

According to Eqs. (3) and (4), the mean mass transfer flux ($\bar{N}$) can be written as:

$$\bar{N} = K_L \Delta_{LMC} \tag{5}$$

At the same time, the total volume of microchannel can be defined as follows:

$$V = \pi H\left(R_2^2 - R_1^2\right) \tag{6}$$

Assuming that the equilibrium concentration of scandium in the organic phase at the inlet equals the outlet, then the result can be written as:

$$C^*_{O,i} = C^*_{O,o} \tag{7}$$

Moreover, the concentration of scandium in the organic phase at the inlet is equal to zero, which can be written as:

$$C_{O,i} = 0 \tag{8}$$

From Eqs. (3)–(8) mentioned above, the following equation is used to characterize the overall volumetric mass transfer coefficient $K_L a$ in the extraction process [27,28], which is evaluated using the following expression:

$$K_L a = \frac{Q_O}{\pi H\left(R_2^2 - R_1^2\right)} \ln \frac{C^*_{O,o}}{C^*_{O,o} - C_{O,o}} \tag{9}$$

3.1. Effect of pH of aqueous phase

In this experiment, the method of conventional stirring was used to explore the extraction mechanism. 100 mL aqueous phase solution with a certain pH and 40 mL organic phase solution was added to a 250 mL beaker, then the mixed fluids were mechanically stirred for 0.5 h with the speed of 300 rpm at 50°C to achieve extraction equilibrium.

The extraction mechanism of scandium with EHEHPA perhaps was consistent with the cation exchange [29], due to the dissociable H^+ ions EHEHPA contained. The extraction equilibrium mechanism can be described as follows:

$$Sc^{3+}_{(A)} + \left(HR\right)_{n(O)} \rightleftharpoons \left(ScH_{n-m}R_n\right)^{(3-m)+}_{(O)} + mH^+_{(A)} \quad (10)$$

The apparent equilibrium constant K_{ex} can be described as follows:

$$K_{ex} = \frac{\left[\left(ScH_{n-m}R_n\right)^{(3-m)+}\right]_{(O)}\left[H^+\right]^m_{(A)}}{\left[Sc^{3+}\right]_{(A)}\left[\left(HR\right)_n\right]_{(O)}} \quad (11)$$

The distribution coefficient $D_{(O/A)}$ of scandium can be described as follows:

$$D_{(O/A)} = \frac{\left[\left(ScH_{n-m}R_n\right)^{(3-m)+}\right]_{(O)}}{\left[Sc^{3+}\right]_{(A)}} \quad (12)$$

The definition of pH is expressed as:

$$pH = -\lg\left[H^+\right] \quad (13)$$

According to the Eqs. (11)–(13) mentioned above, $\lg D_{(O/A)}$ can be expressed as:

$$\lg D_{(O/A)} = \lg\left\{K_{ex}\left(\left[\left(HR\right)_n\right]\right)_{(O)}\right\} + m\text{pH} \quad (14)$$

The results are shown in Fig. 3a, through the conventional stirring experiment mentioned above. It was clear that the number of solvent molecules of EHEHPA in the extraction of the complex was equal to 0.5. The extraction mechanism of scandium with EHEHPA at the range of pH from 1.0 to 2.0 could be obtained as follows:

$$2Sc^{3+}_{(A)} + \left(HR\right)_{2n(O)} \rightleftharpoons \left(Sc_2H_{2n-1}R_{2n}\right)^{5+}_{(O)} + H^+_{(A)} \quad (15)$$

As can be seen from Fig. 3b, it is obvious that increased pH could promote the extraction efficiency of scandium at the range of pH from 0.5 to 3.5. However, the percentage extraction reached the lowest as the pH was equal to 0.5. It could be explained that there was an inhibitory effect on the extraction reaction with the high concentration of H^+ ions.

3.2. Effect of outer-inner rotor distance (D)

Different extraction performances could be clearly obtained by controlling the size of the inner rotor of the rotating microchannel reactor. As shown in Fig. 4, E, η and K_La were significantly improved with the decreased outer-inner rotor distance. The boundary layer of the water–oil two phases was damaged by sheer force and resulted in a smaller interface area when the outer-inner rotor distance increased. However, the sheer force generated by the inner rotor was not strong enough to ensure that the two phases fully contact if the distance was very large, then resulting in the reduction of extraction efficiency. As the distance decreased, the shear force would get stronger due to the smaller microchannel size which had a significant effect on the mass transfer coefficient. In addition, the decrease of the average diameter of the droplet in the smaller distance led to the larger interface area. The smaller the microchannel size was, the stronger the effect of internal circulation would be. The smaller size enhanced the convective mass transfer process and promoted the interface renewal rate which accelerated the interface diffusion rate, thus increasing the extraction efficiency [30].

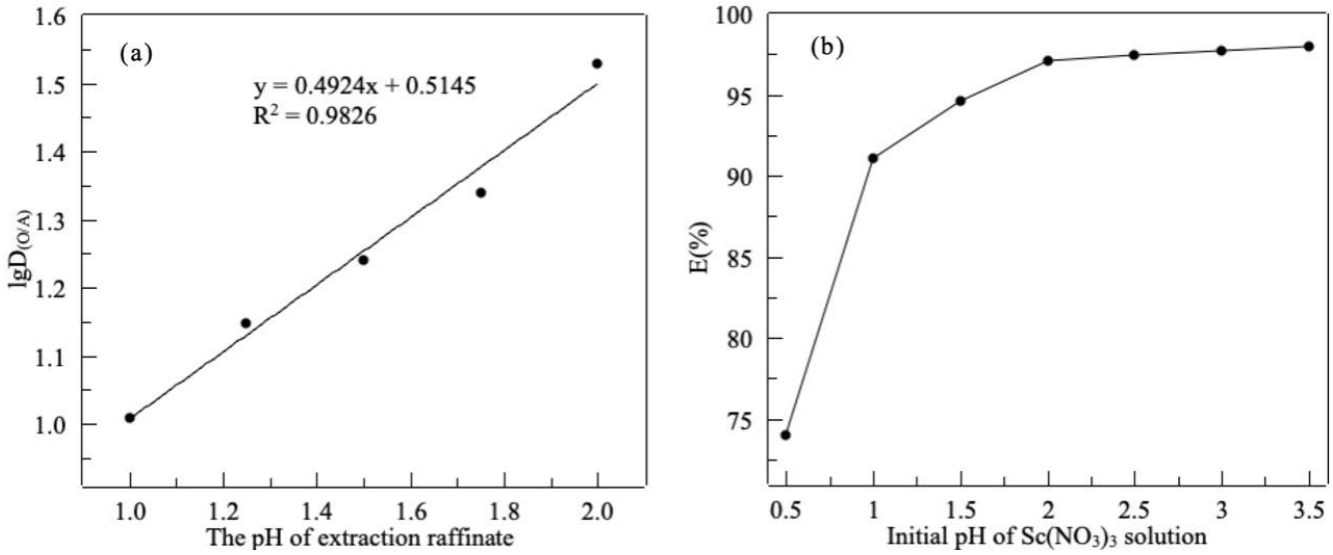

Fig. 3. Effect of initial pH of water phase on (a) $\lg D_{(O/A)}$ and (b) percentage extraction. Conditions: O/A = 0.4; t = 0.5 h; T = 50°C; initial concentration of scandium = 470 mg/L.

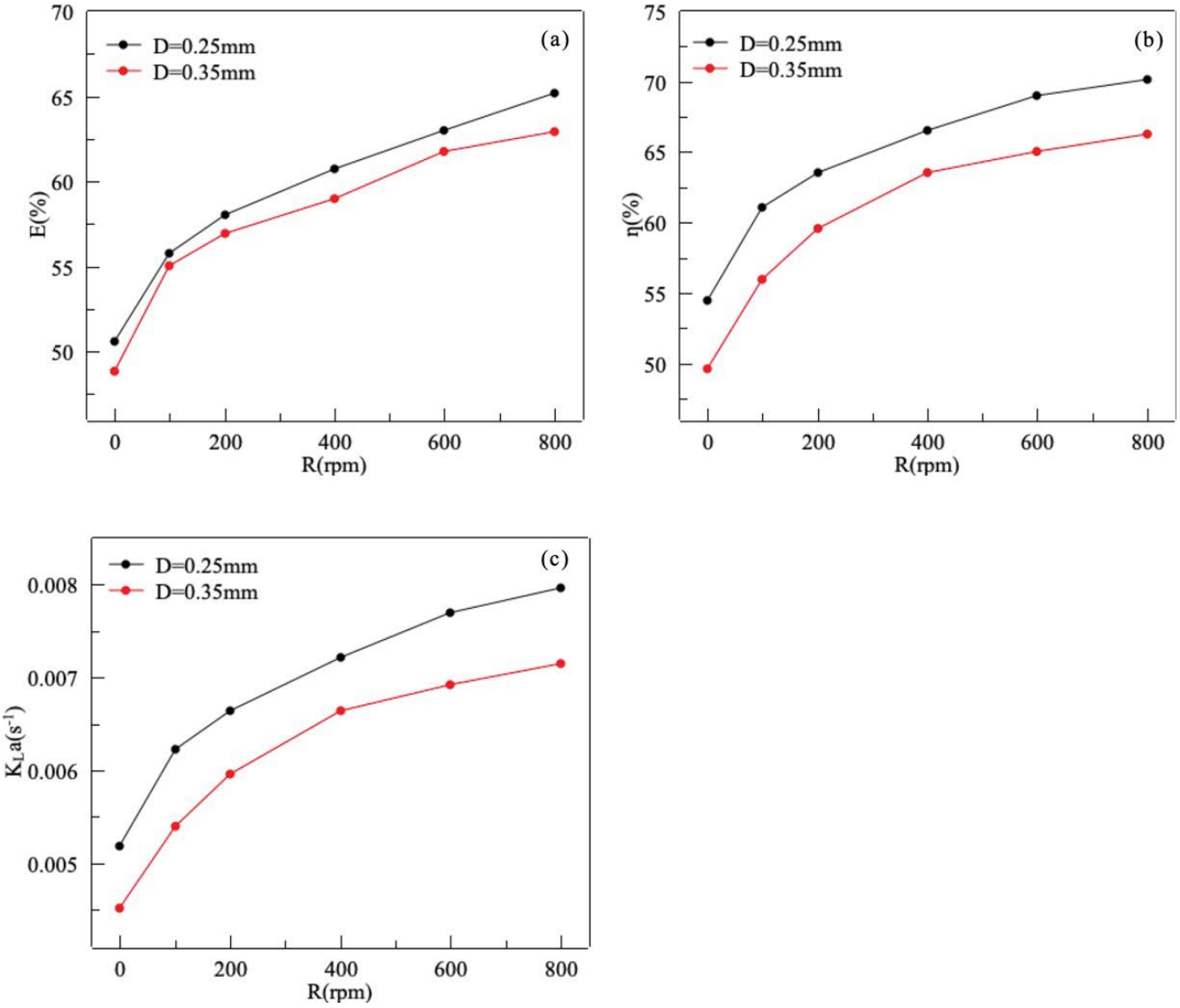

Fig. 4. Effect of outer-inner rotor distance on (a) percentage extraction, (b) percentage stage efficiency, and (c) overall volumetric mass transfer coefficient. Conditions: H = 200 mm; Q_O = 1.2 mL/min; Q_A = 3.0 mL/min; T = 25°C; initial concentration of scandium = 470 mg/L; pH = 3.50.

3.3. Effect of the height of inner rotor (H)

Generally, the residence time of the two-phase fluids in the microchannel reactor would be prolonged with the increase of the height of the inner rotor (H). Fig. 5a and b show the influence of residence time of two-phase fluids on the extraction performance. The results showed that the extraction efficiency was positively correlated with residence time. As shown in Fig. 5c, the smaller the height was, the larger the overall volumetric mass transfer coefficient K_La was. It could be explained that residence time played a major role in liquid–liquid two-phase extraction rather than the mass transfer process.

As the inner rotor remained stationary, the effect of the height of the inner rotor on the extraction performance was very similar. Since the flow pattern of the liquid–liquid two phases in the microchannel reactor was stable parallel flow, the mass transfer performance was not very obvious. With the increase of speed, the effect of the height of the inner rotor on extraction performance became more and more palpable. It could be demonstrated that the height of the inner rotor, that was residence time, had an important influence on the extraction efficiency.

3.4. Effect of speed of the inner rotor (R)

The speed of the inner rotor also showed great influence on the mass transfer performance. When the rotational speed increased, the mixing process of two-phase fluids in the microchannel reactor became intensified. As shown in Fig. 5, the extraction efficiency and overall volumetric mass transfer coefficient gradually increased as the speed of the

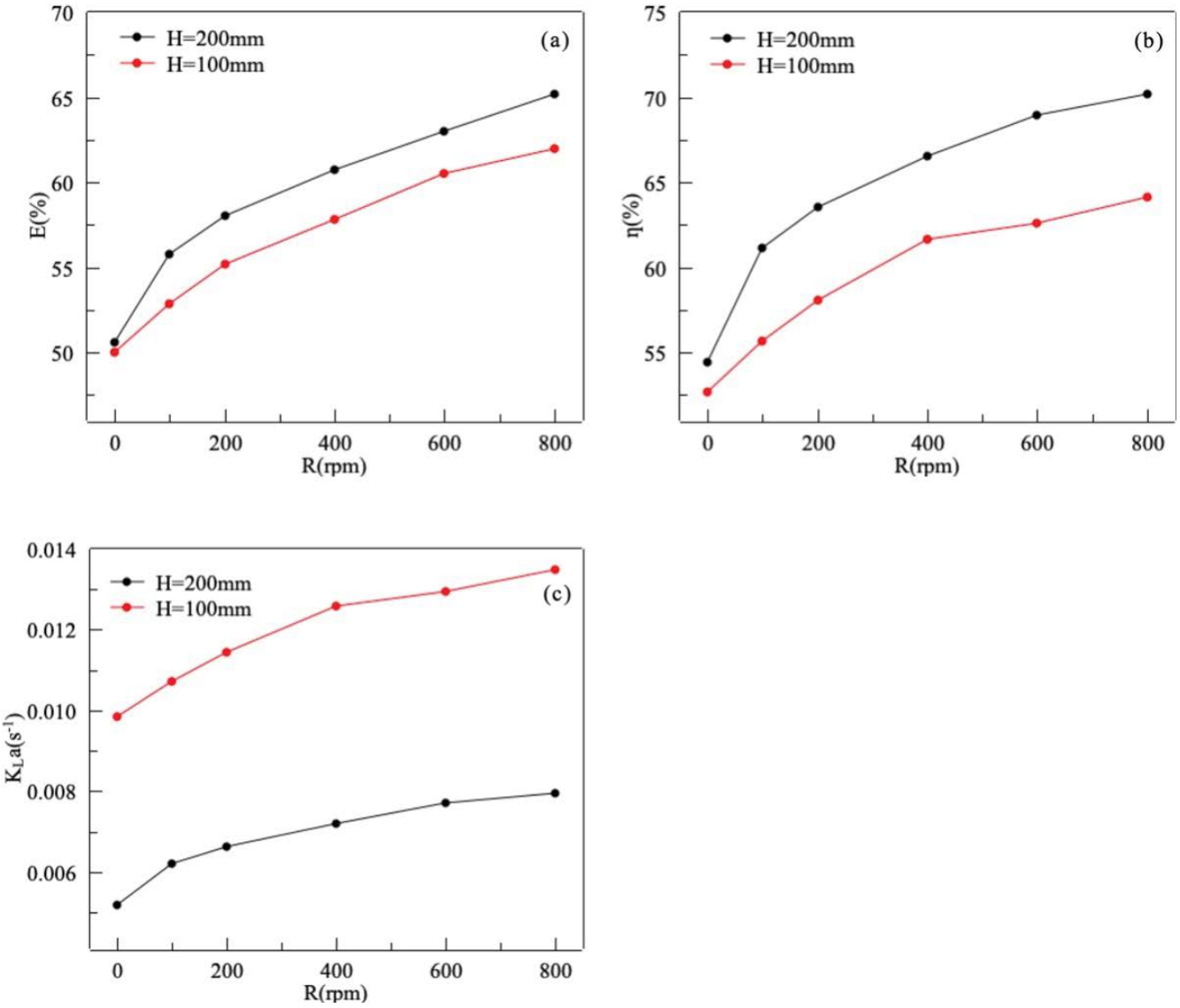

Fig. 5. Effect of the height of inner rotor on (a) percentage extraction, (b) percentage stage efficiency, and (c) overall volumetric mass transfer coefficient. Conditions: R_1 = 9.55 mm; Q_O = 1.2 mL/min; Q_A = 3.0 mL/min; T = 25°C; initial concentration of scandium = 470 mg/L; pH = 3.50.

inner rotor increased from 0 to 800 rpm. Due to the character of the hydrophilic outer cylinder and oleophilic inner rotor, the organic phase and aqueous phase were distributed on the inner rotor and the walls of the outer cylinder under the action of interfacial tension, respectively.

Flow patterns taken by a high-speed camera at different speeds are shown in Fig. 6 (the dark part represents the organic phase and the light part represents the aqueous phase). There was no internal circulation between liquid–liquid two phases and the mass transfer performance was ineffective as the rotational speed was equal to zero. The mass transfer process mainly depended on molecular diffusion [31] due to the stable parallel flow. At low rotational speed, the mass transfer process was primarily controlled by molecular diffusion and the mixing degree of liquid–liquid two phases was not sufficient. The flow patterns of the two phases were more concentrated with the increase of the rotational speed. At the same time, the increased speed enlarged the contact area of two phases and accelerated the interface renewal rate, both of which finally strengthened the mass transfer process, thus enhancing the mass transfer efficiency.

3.5. Effect of the flow velocity of the organic phase (Q_O)

As shown in Fig. 7a and b, as the flow velocity of the organic phase (Q_O) increased from 0.16 to 1.60 mL/min, both E and η decreased while K_La increased gradually. The residence time of the mixed liquids became shorter while the mass transfer area of the two phases increased and the interface renewal rate got accelerated due to the increased flow velocity. Compared with the mass transfer area and

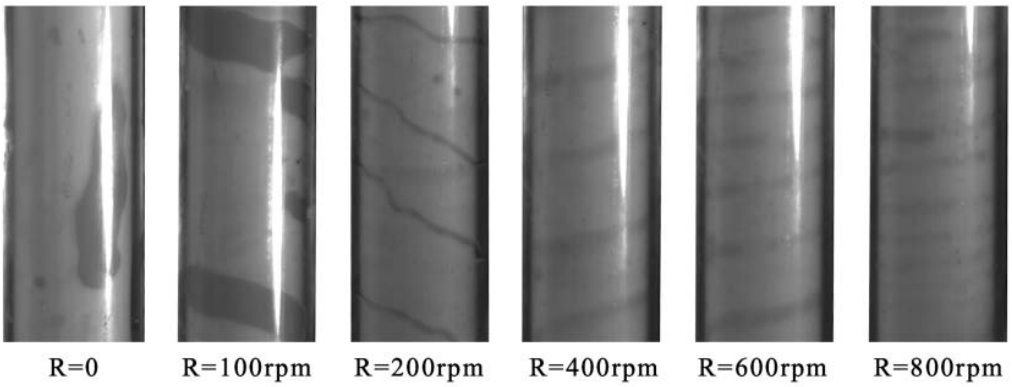

Fig. 6. Variation of flow patterns with the speed of the inner rotor (R). Conditions: R_1 = 9.55 mm; H = 200mm; Q_O = 1.20 mL/min; Q_A = 3.0 mL/min; T = 25°C; initial concentration of scandium = 470 mg/L; pH = 3.50.

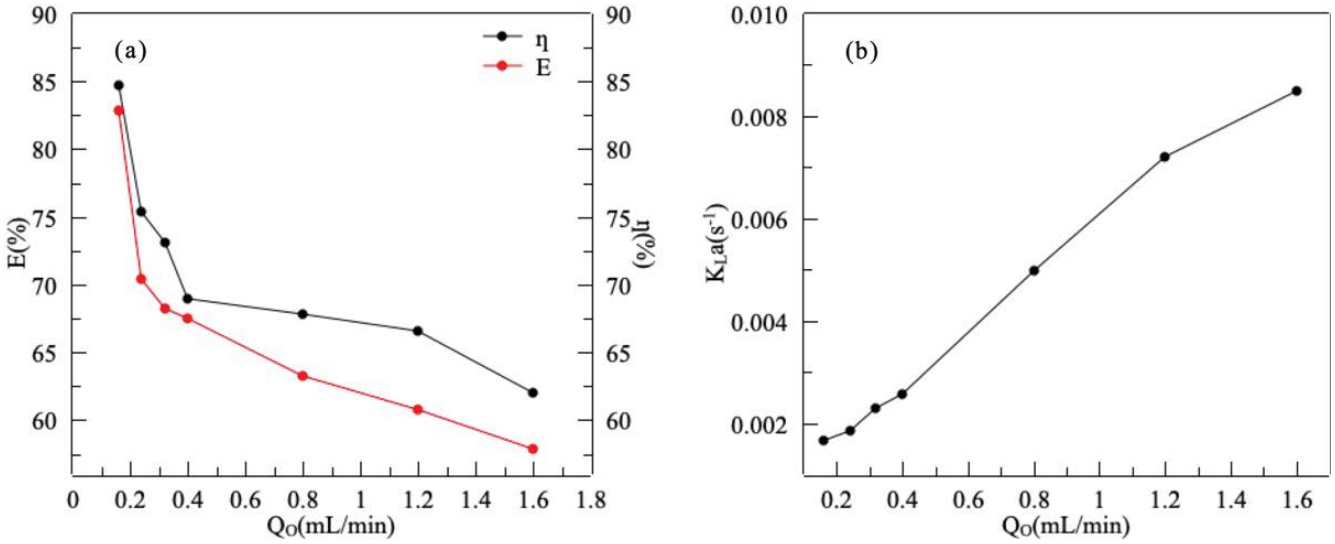

Fig. 7. Effect of the flow velocity of organic phase on (a) percentage extraction and (b) overall volumetric mass transfer coefficient. Conditions: R = 400 rpm; H = 200 mm; R_1 = 9.55 mm; Q_O/Q_A = 0.4; T = 25°C; initial concentration of scandium = 470 mg/L; pH = 3.50.

renewal rate, residence time played a critical role in the mass transfer process.

As shown in Fig. 8, it is obvious that the larger flow velocity lead to the more dispersed organic phase which resulted in the lower extraction efficiency. When Q_O was 0.16 mL/min, E and η reached the maximum, and the decreasing speed gradually slowed down with the increase of Q_O. It indicated that the effects of mass transfer area and renewal rate gradually came into play, while they were not sufficient to replace the residence time which was a more favorable factor for the mass transfer performance. Therefore, it was a more effective way to extract scandium from the aqueous phase by reducing the flow velocity of the organic phase (Q_O).

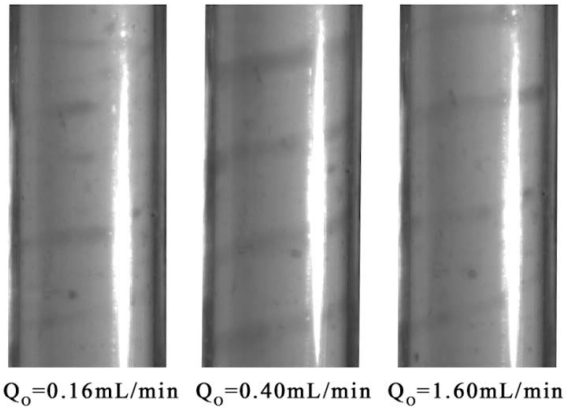

Fig. 8. Effect of flow velocity of organic phase on the flow patterns. Conditions: R = 400 rpm; H = 200 mm; R_1 = 9.55 mm; Q_O/Q_A = 0.4; T = 25°C; initial concentration of scandium = 470 mg/L; pH = 3.50.

3.6. Effect of phase ratio (O/A)

The percentage extraction E and overall volumetric mass transfer coefficient K_La increased with the increase

of phase ratio (O/A) from 0.4 to 0.8 as shown in Fig. 9a and b, respectively. The flow velocity of the aqueous phase remained unchanged and the flow velocity of the organic phase increased gradually, the phase ratio could be changed in this way. In the liquid–liquid two-phase extraction process, the number of ligands provided by the organic phase as the extractant and the interface area also increased correspondingly when the flow velocity of the organic phase increased. However, the increase of the flow velocity would lead to the decrease of the residence time of liquid–liquid two-phase fluids in the microchannel reactor. Residence time, interface area and the number of ligands had distinct effects on the extraction efficiency. It was obvious that interface area and ligands played a dominant role rather than residence time in this experiment. From what has been discussed above, the percentage extraction of scandium from the aqueous phase could be effectively improved by increasing the phase ratio (O/A).

3.7. Reverse extraction

NaOH solution was used for reverse extraction experiment, stirring for 20 min, phase separation in a separation funnel. NaOH concentrations were 0.5, 1, 2, 3 and 4, and the effects of different concentrations of NaOH on the extraction effect were investigated. The reverse extraction curve of Sc^{3+} with different NaOH concentrations is shown in Fig. 10. With the increase of NaOH concentration, the reverse extraction rate of Sc^{3+} increased first and then decreases. It might be that a little white precipitation would appear between the two phases when the concentration of NaOH was too high, and that was unfavorable to the phase separation of scandium hydroxide precipitation generated by reverse extraction. Thus a small amount of precipitate was retained in the organic phase, resulting in the decrease of Sc^{3+} reverse extraction rate. When the concentration of NaOH reached 2 mol/L, the Sc^{3+} stripping rate reached the maximum value.

4. Conclusions

In this work, a rotating microchannel reactor was designed to extract scandium from scandium nitrate aqueous solution with EHEHPA. The explorations of different operating conditions led to the following conclusions:

- Due to the introduction of centrifugal force and materials with different hydrophilic and hydrophobic properties, the microchannel reactor could address the issue of emulsification in extraction.

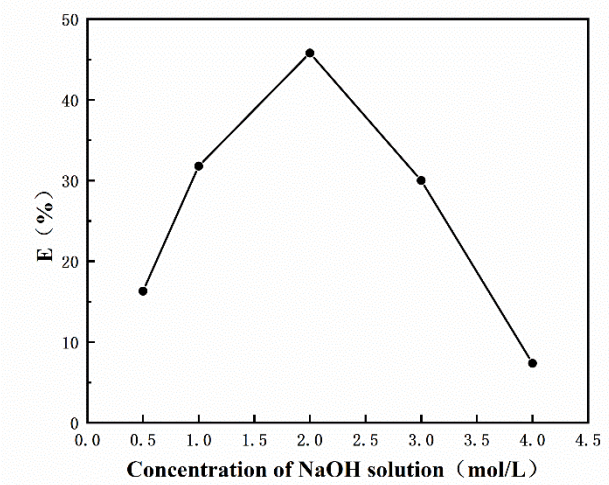

Fig. 10. Effect of NaOH concentration on the reverse extraction. Conditions: Q_O/Q_A = 1:3; T = 25°C; initial concentration of scandium = 430 mg/L; pH = 3.50.

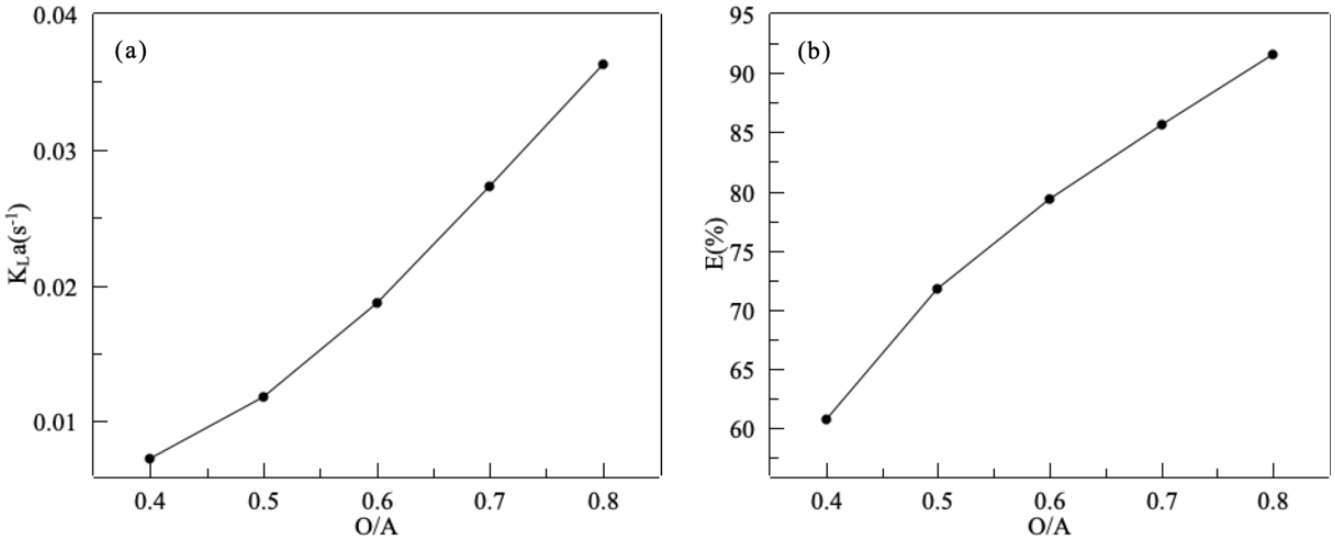

Fig. 9. Effect of phase ratio on (a) overall volumetric mass transfer coefficient and (b) percentage extraction. Conditions: R = 400 rpm; H = 200 mm; R_1 = 9.55 mm; Q_A = 3 mL/min; T = 25°C; initial concentration of scandium = 470 mg/L; pH = 3.50.

- The percentage extraction E increased with pH from 0.5 to 2. There was a strong inhibitory effect on the extraction performance at the lower pH. The extraction mechanism of scandium with EHEHPA could be described as: $2Sc^{3+}_{(A)} + (HR)_{2n(O)} \rightleftharpoons (Sc_2H_{2n-1}R_{2n})^{5+}_{(O)} + H^{+}_{(A)}$.
- The increased speed of the inner rotor (R) could intensify the mixing degree of liquids, the increased height of inner rotor (H) and the decreased flow velocity of the organic phase (Q_O) could extend the residence time in the microchannel reactor, the decreased distance of outer-inner rotor (D) could enlarge the interface area, and the increased phase ratio (O/A) could increase the ligands provided by organic phase. All of the mentioned above could effectively improve the extraction performance. The optimal process conditions were obtained: EHEHPA/kerosene as the extraction organic phase, the concentration of HEHPEHE was 2%, the pH of the aqueous solution was 2, the outer-inner rotor distance (D) was 0.25 mm, the height of inner rotor (H) was 200 mm, the speed of the inner rotor (R) was 800 rpm, and the flow velocity of the organic phase (Q_O) was 0.2 mL/min, the extraction ratio (O/A) was 4:5. Under these conditions, the Sc^{3+} removal rate in the simulated aqueous phase exceeded 97%.

Acknowledgment

The authors gratefully acknowledge financial support from the Chinese National Natural Science Foundation (21776181), the Special Project of Building World-Class Universities (2030704401004), and the Special Fund Project for Cooperation between Sichuan University and Panzhihua City (2018CDPZH-21).

Symbols

$C_{O,o}$	—	Concentration of scandium in the organic phase at the outlet, kg/m^3
$C_{O,i}$	—	Concentration of scandium in the organic phase at the inlet, kg/m^3
$C_{A,o}$	—	Concentration of scandium in the aqueous phase at the outlet, kg/m^3
$C_{A,i}$	—	Concentration of scandium in the aqueous phase at the inlet, kg/m^3
$C^*_{O,e}$	—	Equilibrium concentration of scandium in the organic phase, kg/m^3
$C^*_{O,i}$	—	Equilibrium concentration of scandium in the organic phase at the inlet, kg/m^3
$C^*_{O,o}$	—	Equilibrium concentration of scandium in the organic phase at the outlet, kg/m^3
Q_A	—	Flow velocity of aqueous phase, m^3/s
Q_O	—	Flow velocity of organic phase, m^3/s
K_L	—	Mass transfer coefficient, m/s
K_d	—	Phase equilibrium constant
a	—	Specific interfacial area, m^{-1}
K_La	—	Overall volumetric mass transfer coefficient, s^{-1}
E	—	Percentage extraction, %
$\bar{N}$	—	Mean mass transfer flux, kg/(m^2·s)
V	—	Total volume of the microchannel, L
HR	—	Existence as a dimer EHEHPA in organic phase
n	—	Aggregation number of EHEHPA
m	—	Number of solvent molecules of EHEHPA in extraction of complex
K_{ex}	—	Apparent equilibrium constant
$D_{(O/A)}$	—	Distribution coefficient
D	—	Outer-inner rotor distance, m
H	—	Height of inner rotor, m
R	—	Speed of inner rotor, rad/s
R_1	—	Radius of inner rotor, m
R_2	—	Radius of outer cylinder, m
R_3	—	Radius of aqueous phase inlet, m
R_4	—	Radius of organic phase inlet, m
R_5	—	Radius of mixed phases outlet, m
T	—	Temperature, °C

Greek letters

Δ_{LMC}	—	Log mean concentration difference, kg/m^3
η	—	Percentage stage efficiency, %

References

[1] D. Zou, H. Li, J. Chen, D. Li, Recovery of scandium from spent sulfuric acid solution in titanium dioxide production using synergistic solvent extraction with D2EHPA and primary amine N1923, Hydrometallurgy, 197 (2020) 105463, doi: 10.1016/j.hydromet.2020.105463.
[2] F. Meng, X. Li, L. Shi, Y. Li, F. Gao, Y. Wei, Selective extraction of scandium from bauxite residue using ammonium sulfate roasting and leaching process, Miner. Eng., 157 (2020) 106561, doi: 10.1016/j.mineng.2020.106561.
[3] B. Onghena, C.R. Borra, T. Van Gerven, K. Binnemans, Recovery of scandium from sulfation-roasted leachates of bauxite residue by solvent extraction with the ionic liquid betainium bis(trifluoromethylsulfonyl)imide, Sep. Purif. Technol., 176 (2017) 208–219.
[4] C. Liu, L. Chen, J. Chen, D. Zou, Y. Deng, D. Li, Application of P507 and isooctanol extraction system in recovery of scandium from simulated red mud leach solution, J. Rare Earths, 37 (2019) 1002–1008.
[5] N. Van Nguyen, A. Iizuka, E. Shibata, T. Nakamura, Study of adsorption behavior of a new synthesized resin containing glycol amic acid group for separation of scandium from aqueous solutions, Hydrometallurgy, 165 (2016) 51–56.
[6] K. Wang, G. Luo, Microflow extraction: a review of recent development, Chem. Eng. Sci., 169 (2017) 18–33.
[7] Y.B. Wang, J. Li, Y. Jin, J.H. Luo, Y. Cao, M. Chen, Liquid–liquid extraction in a novel rotor-stator spinning disc extractor, Sep. Purif. Technol., 207 (2018) 158–165.
[8] P. Angeli, D. Tsaoulidis, W. Hashi Weheliye, Studies on mass transfer of europium(III) in micro-channels using a micro laser induced fluorescence technique, Chem. Eng. J., 372 (2019) 1154–1163.
[9] G.L. Mo, H. Liu, S. Dai, Y.B. Wang, J. Li, J.H. Luo, Extraction of Fe^{3+} from NaH_2PO_4 solution in a spiral microchannel device, Chem. Eng. Process. Process Intensif., 144 (2019) 107654, doi: 10.1016/j.cep.2019.107654.
[10] T. Xie, M. Chen, C. Xu, J. Chen, High-throughput extraction and separation of Ce(III) and Pr(III) using a chaotic advection microextractor, Chem. Eng. J., 356 (2019) 382–392.
[11] F. Jiang, J. Pei, S. Yin, L. Zhang, J. Peng, S. Ju, J.D. Miller, X. Wang, Solvent extraction and stripping of copper in a Y-Y type microchannel reactor, Miner. Eng., 127 (2018) 296–304.
[12] S.K. Kurt, I. Vural Gürsel, V. Hessel, K.D.P. Nigam, N. Kockmann, Liquid–liquid extraction system with microstructured coiled flow inverter and other capillary setups for single-stage extraction applications, Chem. Eng. J., 284 (2016) 764–777.
[13] E. Abraham, G.N. Mukunthan Sulochana, B. Soundarajan, S. Narayanasamy, Experimental investigation on microfluidic

reactive extraction of citric acid using trioctylamine/1-decanol system in uniform and nonuniform circular microchannels, Ind. Eng. Chem. Res., 56 (2017) 10845–10855.
[14] Y. Su, N.J. Straathof, V. Hessel, T. Noel, Photochemical transformations accelerated in continuous-flow reactors: basic concepts and applications, Chemistry, 20 (2014) 10562–10589.
[15] L. Zhang, X. Wang, J. Zou, Y. Liu, J. Wang, Effects of an 11-nm DMSA-coated iron nanoparticle on the gene expression profile of two human cell lines, THP-1 and HepG2, J. Nanobiotechnol., 13 (2015) 1–17.
[16] C. Holtze, Large-scale droplet production in microfluidic devices—an industrial perspective, J. Phys. D: Appl. Phys., 46 (2013) 114008.
[17] A. Matsuoka, K. Noishiki, K. Mae, Experimental study of the contribution of liquid film for liquid–liquid Taylor flow mass transfer in a microchannel, Chem. Eng. Sci., 155 (2016) 306–313.
[18] K. Muijlwijk, I. Colijn, H. Harsono, T. Krebs, C. Berton-Carabin, K. Schroën, Coalescence of protein-stabilised emulsions studied with microfluidics, Food Hydrocolloids, 70 (2017) 96–104.
[19] M.C. Morales, J.D. Zahn, Droplet enhanced microfluidic-based DNA purification from bacterial lysates via phenol extraction, Microfluid. Nanofluid., 9 (2010) 1041–1049.
[20] Y. Okubo, T. Maki, N. Aoki, T. Hong Khoo, Y. Ohmukai, K. Mae, Liquid–liquid extraction for efficient synthesis and separation by utilizing micro spaces, Chem. Eng. Sci., 63 (2008) 4070–4077.
[21] R. Ma, C.X. Fan, Y.B. Wang, J.H. Luo, J. Li, Y.Z. Ji, Liquid–liquid microextraction in a rotating microchannel extractor, Chem. Eng. Process. Process Intensif., 151 (2020) 107916, doi: 10.1016/j.cep.2020.107916.
[22] M. Darekar, N. Sen, K.K. Singh, S. Mukhopadhyay, K.T. Shenoy, S.K. Ghosh, Liquid–liquid extraction in microchannels with Zinc–D2EHPA system, Hydrometallurgy, 144–145 (2014) 54–62.
[23] S. Yin, L. Zhang, J. Peng, S. Li, S. Ju, L. Zhang, Microfluidic solvent extraction of La(III) with 2-ethylhexyl phosphoric acid-2-ethylhexyl ester (P507) by a microreactor, Chem. Eng. Process. Process Intensif., 91 (2015) 1–6.
[24] Z. Chen, W.-T. Wang, F.-N. Sang, J.-H. Xu, G.-S. Luo, Y.-D. Wang, Fast extraction and enrichment of rare earth elements from waste water via microfluidic-based hollow droplet, Sep. Purif. Technol., 174 (2017) 352–361.
[25] C. Xu, T. Xie, Review of microfluidic liquid–liquid extractors, Ind. Eng. Chem. Res., 56 (2017) 7593–7622.
[26] S. Dai, J. Luo, J. Li, X. Zhu, Y. Cao, S. Komarneni, Liquid–liquid microextraction of Cu^{2+} from water using a new circle microchannel device, Ind. Eng. Chem. Res., 56 (2017) 12717–12725.
[27] Q. Li, P. Angeli, Intensified Eu(III) extraction using ionic liquids in small channels, Chem. Eng. Sci., 143 (2016) 276–286.
[28] J.B. Modak, A. Bhowal, S. Datta, Extraction of dye from aqueous solution in rotating packed bed, J. Hazard. Mater., 304 (2016) 337–342.
[29] S. Dai, J.H. Luo, J. Li, X.H. Zhu, Y. Cao, S. Komarneni, Liquid–liquid microextraction of Cu^{2+} from water using a new circle microchannel device, Ind. Eng. Chem. Res., 56 (2017) 12717–12725.
[30] S.K. Kurt, F. Warnebold, K.D.P. Nigam, N. Kockmann, Gas–liquid reaction and mass transfer in microstructured coiled flow inverter, Chem. Eng. Sci., 169 (2017) 164–178.
[31] F. Visscher, J. van der Schaaf, M.H.J.M. de Croon, J.C. Schouten, Liquid–liquid mass transfer in a rotor–stator spinning disc reactor, Chem. Eng. J., 185–186 (2012) 267–273.